

Performance demonstration of a compact, single optical frequency Cesium beam clock for space applications

S. Lecomte*, M. Haldimann, R. Ruffieux, P. Berthoud

Observatoire de Neuchâtel

Rue de l'Observatoire 58

CH-2000 Neuchâtel, Switzerland

**Electronic address: steve.lecomte@ne.ch*

P. Thomann

Laboratoire Temps-Fréquence, Université de Neuchâtel

Rue A.-L. Breguet 1

CH-2000 Neuchâtel, Switzerland

Observatoire de Neuchâtel has developed a compact optically-pumped cesium beam frequency standard in the frame of an ESA-ARTES 5 project. The simplest optical scheme, which is based on a single optical frequency for both preparation and detection processes of atoms, has been chosen to fulfill reliability constraints of space applications. With the last evolution of our laboratory demonstrator, we have measured a frequency stability of $\sigma_y = 1.14 \times 10^{-12} \tau^{-1/2}$, which is compliant with the Galileo requirement and our frequency stability goal of $\sigma_y = 1 \times 10^{-12} \tau^{-1/2}$. Present performance limitations are discussed and further improvements are proposed to possibly increase the frequency stability.

I. INTRODUCTION

Several space applications like navigation systems, telecommunications, long-term missions, and scientific missions require onboard atomic clocks. The system capability is mainly defined by the atomic clock performance. Although standard microwave atomic clock technology is well mastered for ground systems, they have to be adapted to the space environment in order to exhibit similar performances with rugged packaging and high system reliability as well as with strong reductions of mass, volume, and power consumption.

The two atomic clocks foreseen to take place onboard the first generation of Galileo satellites are respectively the Passive Hydrogen Maser (PHM) and the Rubidium Atomic Frequency Standard (RAFS). While the RAFS is a very compact clock (2.4 litres, 3.4 kg), the PHM is bigger (26 litres, 18 kg) [1], but exhibits a 5-fold improvement of the long-term frequency stability σ_y ($< 10^{-14}$ for $\tau > 10^4$ s). These two frequency standards being operated in vapour cell conditions, the influence of the environment is dramatic (frequency temperature coefficient). To overcome the long-term frequency instability of these standards, the atomic-beam frequency standard is an elegant alternative presently in wide use for GPS and GLONASS. Compared to a magnetically-deflected Cesium atomic-beam clock, a laser-pumped resonator has a better short-term stability, owing to the fact that it makes use of the full atomic velocity

distribution and of the 2-fold increase of the useful atoms due to optical pumping. It can even compete with the PHM in terms of frequency stability. Moreover, due to its inherently simple design, its manufacturing and its reliability can be strongly improved with respect to the PHM.

Observatoire de Neuchâtel (ON) has developed such an Optically-pumped Space Cesium Atomic Resonator (OSCAR) prototype in the frame of an ESA-ARTES 5 project. Our goal was to demonstrate a frequency stability of $\sigma_y \leq 1 \times 10^{-12} \tau^{-1/2}$ with a compact atomic resonator and only one optical frequency. This choice is motivated by space application prerequisites and has already been discussed [2]. The best-measured frequency stability with a 1-frequency scheme is $\sigma_y = 4 \times 10^{-12} \tau^{-1/2}$ with a compact laboratory atomic resonator and a single laser diode (852 nm, 25-MHz linewidth) [3]. By also using a compact atomic resonator, but a more complex optical setup (2-frequency scheme: one laboratory extended-cavity diode laser and one acousto-optic modulator), the frequency stability was improved to $\sigma_y = 1.4 \times 10^{-12} \tau^{-1/2}$ using either a Cs beam [4,5] or a Rb beam [6].

In these proceedings, we report on developments of our compact atomic resonator. First we describe the experimental setup (§II), then we present the experimental results and discuss the current limitations to the frequency stability performances (§III.A and III.B). Finally we present solutions to improve the atomic resonator frequency stability in the conclusion (§IV).

II. EXPERIMENTAL SETUP

The architecture of the frequency standard is shown in Fig. 1: the Physics Package (PP) is composed of the Atomic Resonator (AR), while the Opto-Electronics Package (OEP) contains the Optics and Laser module (OL), the Optics and Laser Control module (OLC) and the Atomic Resonator Control module (ARC).

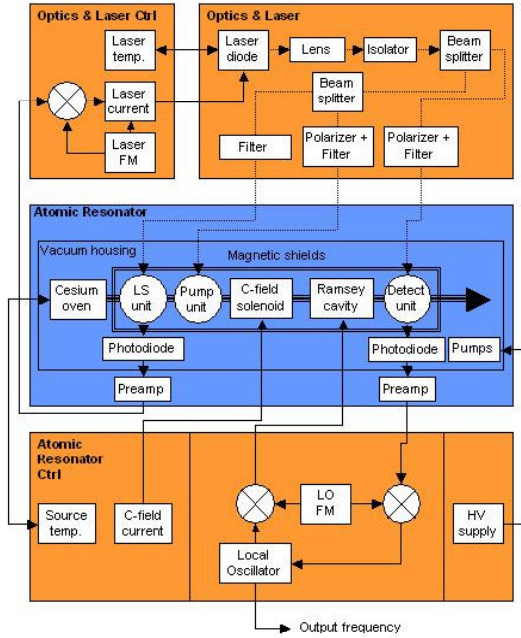


Fig. 1: Block diagram of the Optically-pumped Space Cesium Atomic Resonator (OSCAR). The blue module in the middle is the Physics Package and the orange side modules are parts of the Opto-Electronics Package and of the Atomic Resonator Control module.

The AR is fairly standard for an optically-pumped atomic beam resonator. An oven containing 2g of Cesium, fitted with a multi-channel collimator, produces the atomic beam. It crosses a first laser beam in the Laser Stabilization Unit (LSU), which takes advantage of the fluorescence signal to stabilize the laser frequency. Then, the atomic beam propagates through a second zone to achieve the required ground state population inversion (Pumping Unit, PU). Subsequently, the atomic beam crosses a short Ramsey cavity (12 cm), where the microwave resonance takes place. Finally, the atomic beam crosses the third laser beam (generated by the same laser) in the Detection Unit (DU), in which the final atomic state is optically probed. In both the LSU and in the DU, the atomic beam fluorescence light is first collected by a specially-machined concave mirror, then converted into photo-currents by a Si photodiode (33 mm²) placed under vacuum, and finally converted into a photo-voltage by a low noise pre-amplifier outside of the vacuum enclosure. The three optical units and the microwave cavity are surrounded by a solenoid coil which produces a uniform magnetic C-field (up to 100 mG). The AR is maintained under ultra high vacuum by Cesium getters (graphite) and by a commercial ion pump.

The OL has been assembled to operate the atomic resonator with the 1-frequency scheme. Note however that it could be easily adapted for the 2-frequency scheme, by simply adding an acousto-optic modulator to shift the frequency of the laser detection beam.

The optical beam propagates in free space. The single 852-nm laser source is a Distributed Feed-Back diode (DFB), with

an output power > 15 mW and a spectral linewidth < 2 MHz. The diverging laser beam is first collimated, then isolated (40 dB), and finally split into three beams. Neutral density filters and polarisers properly prepare their respective power and polarisation before entering the AR by windows. A homemade external cavity diode laser with a wavelength of 894 nm has also been used in place of the 852-nm DFB laser, due to the lack of performing DFB laser at this wavelength.

The ARC is composed of the necessary power supplies and driving electronics for the Cs oven temperature regulation, for the C-field solenoid current provision and for the ion pump high voltage supply. The microwave frequency chain (local oscillator, frequency multiplier and phase modulator) is a commercial device. It is based on the multiplication of a 10-MHz quartz oscillator with a step recovery diode. The frequency locking of the quartz oscillator and of the laser diode are performed digitally in a single Digital Signal Processor (DSP). In addition, the C-field amplitude and the RF interrogation power servo-loops can be implemented sequentially with the quartz frequency servo loop. Their different relevant parameters such as modulation amplitudes, gains, duty cycle and filter topologies can be adapted very conveniently with this digital electronics. Moreover it offers additional capabilities such as automatic atomic line searching, which however has not yet been implemented.

The OLC uses the Cesium beam inside the AR as the frequency discriminator (LSU photo-detector). The laser frequency is modulated by its injection current at 10 kHz and locked on the pumping transition lines Cs D2:44' σ (wavelength \approx 852 nm) or Cs D1:34' π (wavelength \approx 894 nm) by synchronous detection. These hyperfine transitions have been chosen for their highest population inversion ratio $\eta = 15.5\%$ and $\eta = 14.4\%$ respectively, and for its high fluorescence yield $\Delta_{ph} = 2.4$ ph/at [7]. Note that both transitions have nearly the same clock relevant parameters ($\eta \cdot \Delta_{ph}$).

III. EXPERIMENTAL RESULTS

Before investigating optically the atomic beam, we have calibrated its overall flux with an ionization detector located downstream of the atomic resonator. Its detection solid angle is 6×10^{-5} sr (open surface of 5.5 mm² at a distance of 301 mm from the oven). The flux has been measured for oven temperatures from 90°C to 130°C. The measured ion current (proportional to the atomic flux) increases as the calculated Cs vapor density up to 100°C. For higher temperature, the atomic flux starts to saturate with respect to the Cs vapor density, which indicates the transition from molecular flow to viscous flow in the collimator. This behavior is similar to the one observed previously [8]. The useful atomic flux for the atomic resonator (atoms in the $m_F = 0$ hyperfine state having contributed to the Ramsey signal) is about 1.5×10^{10} at/s at the oven temperature of 130°C.

The two fluorescence light collection optics with 33-mm² silicon photodiodes convert about 30% of the fluorescence photons into photoelectrons. This collection efficiency is presently limited by the size of the photodetectors. It could be

increased by increasing the photodetectors size but at the price of more stray light and its associated shot-noise.

Birefringent optical elements depolarize the laser beams in the PU and the DU [9] for the used D2 transition. A polarization gradient along the atomic beam increases the efficiency of the optical pumping in the PU without requiring a strong static magnetic field [10], or a 1D optical molasses [11].

The optical power in both the PU and DU was optimized for maximum signal-to-noise ratio (SNR) in order to increase the frequency stability of the standard.

A. Results obtained with the D2:44' σ transition

The central Ramsey fringe recorded at an oven temperature of 130°C is plotted in Fig. 2. A weak and uniform C-field of 52 mG is applied over all optical units (LSU, PU, and DU) and over the microwave Ramsey cavity (Fig. 1). The RF power is adjusted for maximizing the clock signal. The AR has the following performances: the atomic linewidth is 858 Hz, yielding an atomic quality factor of 10^7 , the Ramsey central fringe peak-to-valley photo-current is 1681 pA, the background photo-current is 2.5 nA, and the noise current density at resonance is 41 fA/Hz^{1/2} (at a Fourier frequency of 27 Hz, see Fig. 3) yielding a clock SNR of 41'000 Hz^{1/2} at clock resonance.

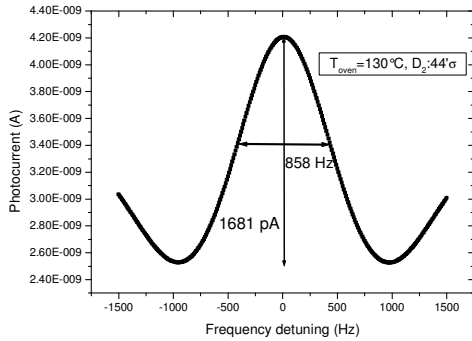


Fig. 2: Ramsey central fringe recorded with an oven temperature of 130°C.

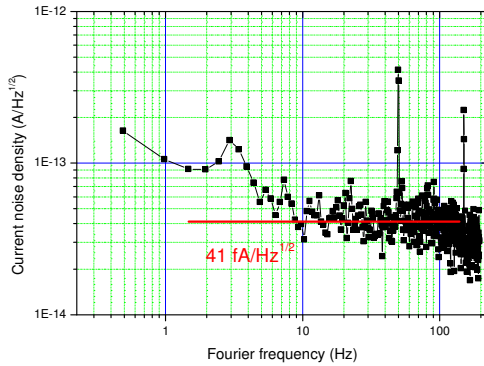


Fig. 3: Current noise density (measured at Ramsey fringe peak) recorded with an oven temperature of 130°C.

By operating the atomic resonator with these optimal parameters, and frequency locking the quartz local oscillator

with the digital electronics, we have measured its frequency stability with respect to an active hydrogen maser (Fig. 4). The Allan standard deviation extrapolated down to 1s gives at short-term frequency stability of $\sigma_y = 1.51 \times 10^{-12} \tau^{-1/2}$. To the best of our knowledge, this frequency stability is the best ever measured with a compact optically-pumped atomic beam frequency standard operated with a single optical frequency scheme (single laser diode and no acousto-optic modulator). For long integration time constants (from 4000s), environmental magnetic and thermal perturbations degrade the clock frequency stability. For this laboratory demonstration, we remind that only one single magnetic shield is assembled. Moreover, neither C-field nor RF power servo loops are operating.

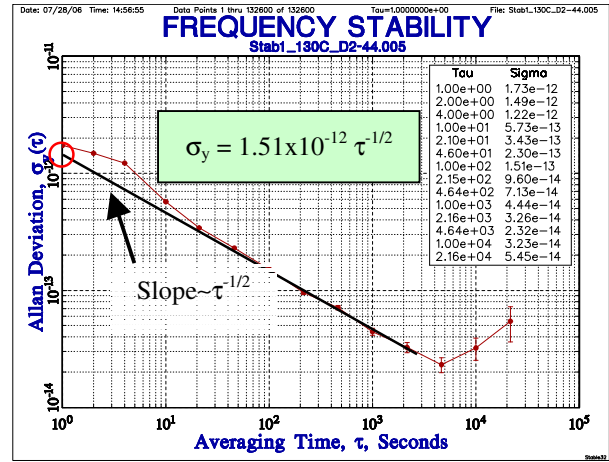


Fig. 4: Measured frequency stability of OSCAR operated with a single wavelength and a 852-nm DFB laser.

Although the stability of the clock is better than the requirement for the Galileo satellite navigation system ($\sigma_y \leq 3 \times 10^{-12} \tau^{-1/2}$), the ultimate frequency stability goal of $\sigma_y \leq 1 \times 10^{-12} \tau^{-1/2}$ has been nearly reached. In fact, the clock noise is not atomic shot-noise limited. In the following we will analyze the various noise contributions to the total clock noise and discuss the improvements to be performed in order to increase the clock SNR and reach the atomic shot-noise limit.

In Fig. 5, we plot the different noise current densities as a function of the Ramsey peak-valley photocurrent. The different noise measurements and the optimizations have been performed at the Ramsey central fringe maximum. The corresponding oven temperatures are given for information.

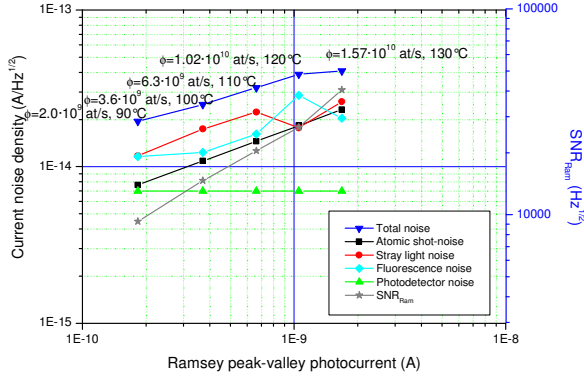


Fig. 5: Noise budget and overall SNR of OSCAR as function of the Ramsey peak-valley photocurrent.

We have identified four noise contributions in the clock signal noise budget:

1. *Photodetector noise*: it is measured in the dark and is independent of the Ramsey photocurrent; for nominal operating atomic flux, this contribution is negligible in the overall noise budget.
2. *Stray light noise*: it is measured with the nominal optical power but off-resonance, is proportional to the square root of the DC stray light level (shot noise), but is independent of the Ramsey photocurrent; this technical noise contribution is mainly due to light scattering by the optical windows mounted on the vacuum enclosure. The optical power has been optimized for each oven temperature and at the peak of the Ramsey central fringe.
3. *Atomic shot-noise*: it is calculated as the square root of the atomic signal; presently this noise contribution is largely dominated by the technical noise.
4. *Fluorescence noise*: it is computed from the total measured noise minus the other contributions in RMS values. This noise contribution appears to be roughly proportional to the square root of the Ramsey signal and is related to the residual frequency noise of the laser converted into amplitude by the atomic beam frequency discriminator. In order to reduce it, the residual frequency noise of the laser has to be minimized in closed loop operation. Presently, our laser stabilization electronics has a very narrow servo-loop bandwidth (<100 Hz), limited by the ADC/DAC stage of our digital electronics. By increasing it by a factor 100, the amount of fluorescence noise should be reduced to an acceptable value. Another alternative, demonstrated here, is to optimize the optical power as function of the atomic flux. An optimum of the optical power, in terms of clock SNR, is found for each atomic flux.

The second major noise contribution arises from the stray light level and its associated shot-noise. While the light traps

placed under vacuum are sufficiently absorbent, the laser scattering on the optical windows of the vacuum enclosure induces a large amount of stray light. New windows of better optical quality with efficient anti-reflection (AR) coating will be mounted and should strongly reduce the amount of stray light. By effectively reducing these two major noise contributions, the total noise of the clock should be close to the atomic shot-noise contribution.

B. Results obtained with the $D1:34' \pi$ transition

The characterization of the resonator has been repeated at 894 nm with a C-field of 83 mG. In this case an extended cavity diode laser with a narrow linewidth was used. By operating the oven at a temperature of 130°C , we obtained a SNR of $43'000 \text{ Hz}^{1/2}$. This narrower laser (compared to the DFB laser) allows to injecting less optical power in the detection unit. This reduces the stray light associated noise and the laser induced fluorescence noise. The clock SNR is therefore increased since the Ramsey peak-valley is nearly the same as with the DFB laser.

The frequency stability of $1.14 \times 10^{-12} \tau^{-1/2}$ measured against a hydrogen maser and presented in Fig. 6 is, to our knowledge, the best stability ever measured for such a resonator. The displayed frequency stability is significantly degraded for integration times $\tau < 100$ s. This is partially due to the C-field current source which was not actively stabilized (it was not the case for the stability presented in Fig. 4). For long integration times $\tau > 1000$ s, environmental perturbations become visible.

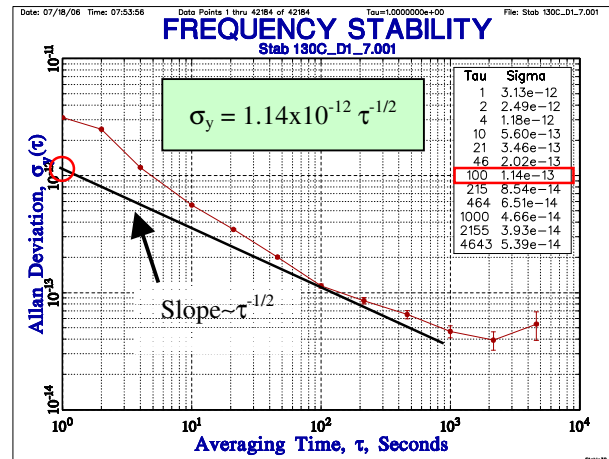


Fig. 6: Measured frequency stability of OSCAR operated with a single wavelength and a 894-nm extended-cavity diode laser.

IV. CONCLUSIONS AND OUTLOOK

We have reported in these proceedings on the experimental setup of an optically-pumped cesium beam frequency standard. Its concept relies on the simplest optical scheme, in which we use only one optical frequency (one laser, no AOM). By depolarizing the laser beams (only for the D2 transition) for the optical pumping processes (preparation and detection), we can use a single, uniform and weak magnetic

C-field for the optical units without trapping atoms in dark states. A fully digital electronics based on a DSP processor has been specially developed for frequency locking both the laser and the quartz local oscillator. This digital electronics also allows to sequentially locking the magnetic C-field and the RF injection power in the Ramsey cavity although it has not been used in the present measurements.

We have demonstrated what is, to the best of our knowledge, the best ever-measured frequency stability of $\sigma_y = 1.14 \times 10^{-12} \tau^{-1/2}$ with a compact optically-pumped atomic beam frequency standard operated with a single optical frequency scheme. Although the demonstrated frequency stability is sufficient for Galileo, the clock SNR is not yet limited by the atomic shot-noise. The noise budget has identified the two major noise sources: the “fluorescence noise” and the “stray light noise”. While the former could be reduced by increasing the laser frequency servo loop bandwidth, the later will call for top quality optical windows. The marginal fluorescence light collection efficiency could be increased by implementing new and optimize optical collectors with possibly larger photodetectors. The results of this study will be implemented in the design of the breadboard Cesium resonator for the second generation of Galileo onboard clocks. This new project is currently ongoing with the financial support of ESA within a consortium led by Thalès Electron Devices, France, and with the following partners: Oerlikon Space AG, Switzerland, SYstème de Référence Temps Espace, France and Observatoire de Neuchâtel [12, 13].

REFERENCES

- [1] F. Droz et al., “The On-board Galileo Clocks: Rubidium Standard and Passive Hydrogen Maser -Current Status and Performance-“, 20th European Time and Frequency Forum, 2006, Braunschweig, Germany.
- [2] P. Berthoud et al., “A feasibility study of an optically-pumped cesium beam resonator for space applications”, 19th European Time and Frequency Forum, 2005, Besançon, France.
- [3] P. Petit et al., “Performance of a 2 dm³ optically pumped cesium beam tube: a progress report”, 8th European Time and Frequency Forum (EFTF), 1994, Munich, Germany.
- [4] R. Lutwak et al., “Optically-pumped cesium beam frequency standard for GPS-III”, 33rd Annual Precise Time and Time Interval (PTTI) Meeting, 2001, Long Beach, CA, USA.
- [5] S. Guérandel et al., “Compact cesium beam frequency standard: improvements of the frequency stability towards the 10-12 t-1/2 level”, 16th European Time and Frequency Forum, 2002, St-Petersburg, Russia.
- [6] A. Besedina et al., “Preliminary results of investigation of the high-stable Rutherfordium atomic beam frequency standard with laser pumping/detection for space”, 20th European Time and Frequency Forum, 2006, Braunschweig, Germany.
- [7] N. Dimarcq et al., “Comparison of pumping a cesium beam tube with D₁ and D₂ lines”, J. Appl. Phys., **69** (3), p. 1158-1162 (1991).
- [8] S. Lecomte et al., “Development of a single-frequency optically-pumped cesium beam resonator for space applications”, 20th European Time and Frequency Forum, 2006, Braunschweig, Germany.
- [9] P. Berthoud and P. Thomann, patent number WO 2006/084829 A1.
- [10] V. Giordano et al., “New design for a high performance optically pumped cesium beam tube”, IEEE Transactions on Ultrasonics, Ferroelectrics, and Frequency Control, **38** (4), p. 350-357 (1991).
- [11] J. H. Shirley and R. E. Drullinger, “Zeeman coherences and dark states in optically pumped cesium frequency standards”, IEEE Prec. Electromagn. Meas., 1994, Boulder, CO, USA.
- [12] S. Guérandel et al., “In-depth analysis of the frequency analysis of optically pumped cesium beam frequency standards”, 21th European Time and Frequency Forum, 2007, Geneva, Switzerland, in these proceedings.
- [13] V. Hermann et al., “OSCC project: a space Cs beam optically pumped atomic clock for Galileo”, 21th European Time and Frequency Forum, 2007, Geneva, Switzerland, in these proceedings.